

Multistability in symmetric chaotic systems

C. Li^{1,a}, W. Hu², J.C. Sprott³, and X. Wang²

¹ School of Electronic and Information Engineering, Nanjing University of Information Science and Technology, Nanjing 210044, China

² College of Electronic and Information Engineering, Nanjing University of Aeronautics and Astronautics, Nanjing 210016, China

³ Department of Physics, University of Wisconsin-Madison, Madison, WI 53706, USA

Received 20 March 2015 / Received in final form 20 May 2015
Published online 27 July 2015

Abstract. Chaotic dynamical systems that are symmetric provide the possibility of multistability as well as an independent amplitude control parameter. The Rössler system is used as a candidate for demonstrating the symmetry construction since it is an asymmetric system with a single-scroll attractor. Through the design of symmetric Rössler systems, a symmetric pair of coexisting strange attractors are produced, along with the desired partial or total amplitude control.

1 Introduction

Multistability poses a threat for engineering systems because the system may unpredictably switch into an undesirable state. Even simple chaotic flows can have such multistable states [1–7]. Systems with a symmetry are especially vulnerable to multistability since any asymmetric attractor is guaranteed to have a twin attractor symmetric with it. However, multistability may have benefits such as allowing one to simulate and study phenomena in the real world where it also occurs.

Amplitude control provides one method for detecting multistability since different initial conditions may lie in different basins of attraction [8]. Furthermore, amplitude control is a key issue for chaos applications in communications and radar engineering because a proper amplifier is difficult to design for the broad-band frequency spectrum [9–11]. Most components in a chaotic circuit affect both the amplitude of the signals and their character, and thus they affect both the amplitude and the bifurcations. Sometimes there are pure amplitude control parameters in chaotic systems, which are physically realized by varying one of the existing resistors in a circuit rather than using additional variable-gain amplifiers. Examples include systems of ordinary differential equations in which all the terms except for one are of the same degree [12–14] or where the system has an involutorial symmetry [13, 14].

Multistability and amplitude control sometimes become entangled in dynamic systems with involutorial symmetry [14]. We can find the phenomenon of multistability accompanied with possible amplitude control in real world directly; however, from the construction of symmetric systems, we can clearly get a good observation of the

^a e-mail: goontry@126.com; chunbiaolee@gmail.com

multistability generated from the symmetrization which also gives various kinds of amplitude control. Furthermore the originally symmetric systems may be globally attracting (all initial conditions approach it) [17], which hides part of their general characteristics. In this paper, construction of symmetric chaotic flows based on the Rössler system are presented as prototypical examples of multistability and amplitude control. In Sect. 2, a rotationally invariant system with a polynomial nonlinearity is designed in which an additional equilibrium point is introduced for multistability. In Sect. 3, an inversion invariant system is obtained by introducing linear feedback and removing some of the polarity information. Independent amplitude parameters are obtained for both cases, allowing partial and total amplitude control. Coexisting strange attractors are observed in the respective basins of attraction. Some conclusions are given in the last section.

2 Multistability in symmetric systems with partial amplitude control

According to the definition of partial amplitude control [13], one can find independent amplitude control parameters in some symmetric flows [14]. However, even in systems without any symmetry, one can often simultaneously obtain multistability and an independent amplitude control parameter. For example, consider the Rössler system [15], which is described by

$$\begin{aligned}\dot{x} &= -y - z \\ \dot{y} &= x + ay \\ \dot{z} &= b + z(x - c).\end{aligned}\tag{1}$$

When $a = b = 0.2, c = 5.7$, the system is chaotic as shown in Fig. 1 with Lyapunov exponents (LEs) of $(0.0714, 0, -5.3943)$ and a Kaplan-Yorke dimension of $D_{KY} = 2.0132$. System (1) has two equilibrium points, $(0.0070, -0.0351, 0.0351)$ and $(5.6930, -28.4649, 28.4649)$ with corresponding eigenvalues $(-5.6870, 0.0970 \pm 0.9952i)$ and $(0.1930, -0.000005 \pm 5.4280i)$, which are spiral saddle points.

Unlike the symmetric Lorenz system [16], the Rössler system is asymmetric. It has seven terms including one constant, one quadratic term, and correspondingly three parameters. Thus it is a good candidate for making symmetric attractors, producing multistability, and providing amplitude control parameters. To construct a symmetric system, the structure can be altered by revising either the linear or nonlinear terms. To construct a rotationally invariant system, consider the system that is invariant under the transformation $(x, y, z) \rightarrow (-x, -y, z)$, corresponding to a 180° rotation about the z -axis. Thus it is necessary to multiply some of the terms in system (1) by appropriate choices of the variables, one example of which is given by

$$\begin{aligned}\dot{x} &= -y - yz \\ \dot{y} &= x + ay \\ \dot{z} &= b + z(x^2 - c).\end{aligned}\tag{2}$$

System (2) also has seven terms and three independent parameters. The dynamic regions in the parameter space of (a, c) at $b = 0.2$ are shown in Fig. 2. In this plot, initial conditions are chosen randomly from a Gaussian distribution centered on the origin with unit variance for each pixel, so that the dotted regions represent candidates for coexistence of different attractor types. When $a = b = 0.2, c = 6.5$, system (2) is chaotic with double peaks as shown in Fig. 3. The corresponding Lyapunov exponents are $(0.1639, 0, -2.7607)$, and the Kaplan-Yorke dimension is $D_{KY} = 2.0594$. The new system (2) now has three equilibrium points, $(0, 0, 0.0308)$ and $(\pm 2.5884, \mp 12.9422, -1)$ with eigenvalues $(-6.5, 0.1 \pm 1.0103i)$ and $(0.2, 0.1 \pm 8.1847i)$, which are spiral saddles. The additional nonlinearities add another equilibrium point

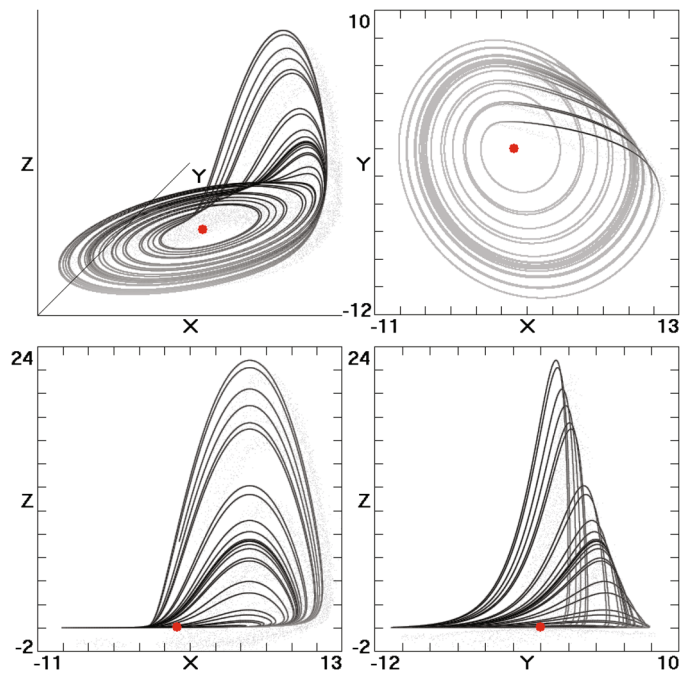


Fig. 1. Four views of the Rössler attractor for $(a, b, c) = (0.2, 0.2, 5.7)$ with initial conditions $(-9, 0, 0)$ in Eq. (1). One of the two equilibrium points is shown as a red dot; the other is off scale.

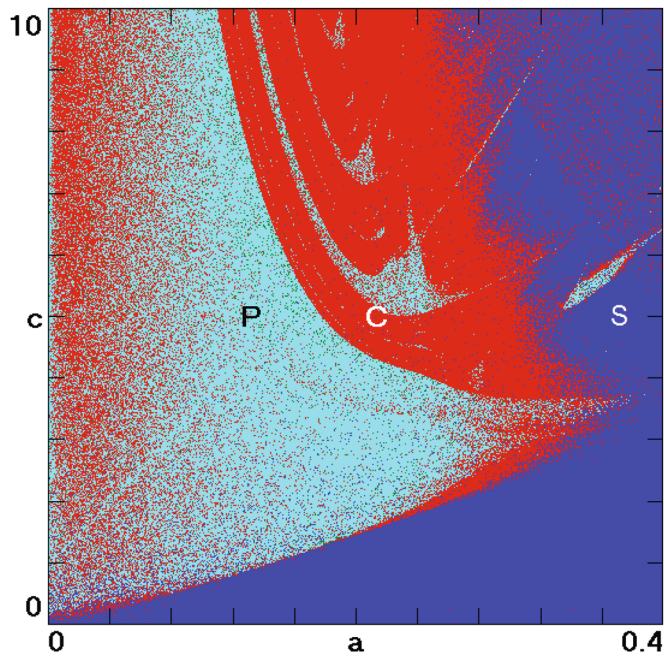


Fig. 2. Regions of various dynamical behaviors for system (2) as a function of the bifurcation parameters a and c with $b = 0.2$. The chaotic and transiently chaotic regions (C) are shown in red, the periodic regions (P) are shown in cyan, and the stable equilibrium regions (S) are shown in dark blue.

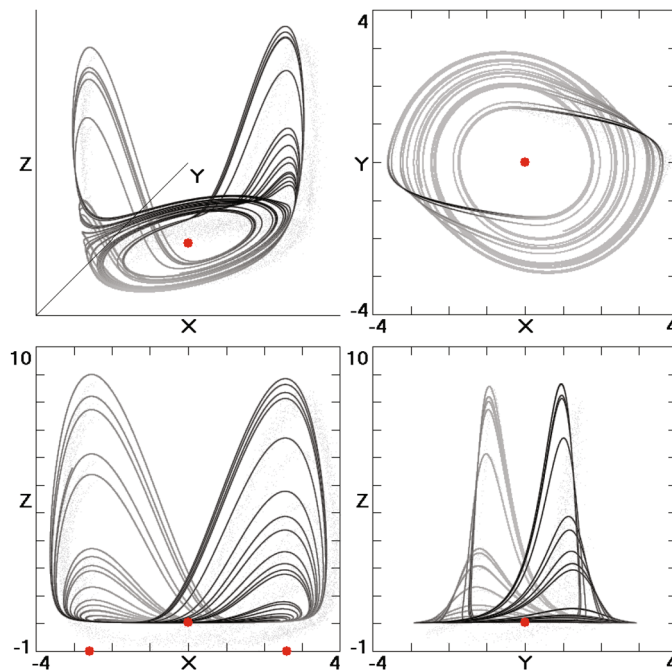


Fig. 3. Four views of the rotationally-symmetric Rössler attractor for $(a, b, c) = (0.2, 0.2, 6.5)$ with initial conditions $(1, 0, 0)$ in Eq. (2). The equilibrium points are shown as red dots.

so that the system has a symmetric pair of equilibria, but the strange attractor is symmetric.

Unlike system (1), this system has one independent partial amplitude control parameter as evidenced by introducing a coefficient h in the cubic term,

$$\begin{aligned}\dot{x} &= -y - yz \\ \dot{y} &= x + ay \\ \dot{z} &= b + z(hx^2 - c).\end{aligned}\quad (3)$$

To show this, let $x = u/\sqrt{h}$, $y = v/\sqrt{h}$, $z = w$ to obtain new equations in the variables u, v, w that are identical to Eq. (2). Therefore, the coefficient h controls the amplitude of the variables x and y according to $1/\sqrt{h}$, while the amplitude of z is unchanged.

In addition to the single symmetric attractor, system (2) can have a symmetric pair of strange attractors. When $a = b = 0.2$, $c = 4.6$, system (2) has coexisting interlinked strange attractors with single peaks as shown in Fig. 4 with basins of attraction as shown in Fig. 5. The basins of attraction for the two chaotic attractors are indicated by light blue and red, respectively, while the white regions of the plot correspond to initial conditions that are unbounded and approach infinity. Generally, we select a cross section going through equilibrium points for observing the dynamics near the critical points, although the section $z = 2$ was chosen here to go through the middle of the attractor. The black lines are cross-sections of the corresponding strange attractors that nearly touch their basin boundaries. The basins have the expected symmetry about the z -axis and a fractal structure. The corresponding Lyapunov exponents for the two coexisting strange attractors are $(0.0724, 0, -1.2974)$, and the Kaplan-Yorke dimension is $D_{KY} = 2.0558$.

With an increase in the parameter c , the two coexisting strange attractors merge into one like the attractor shown in Fig. 3. After merging, there is a periodic window

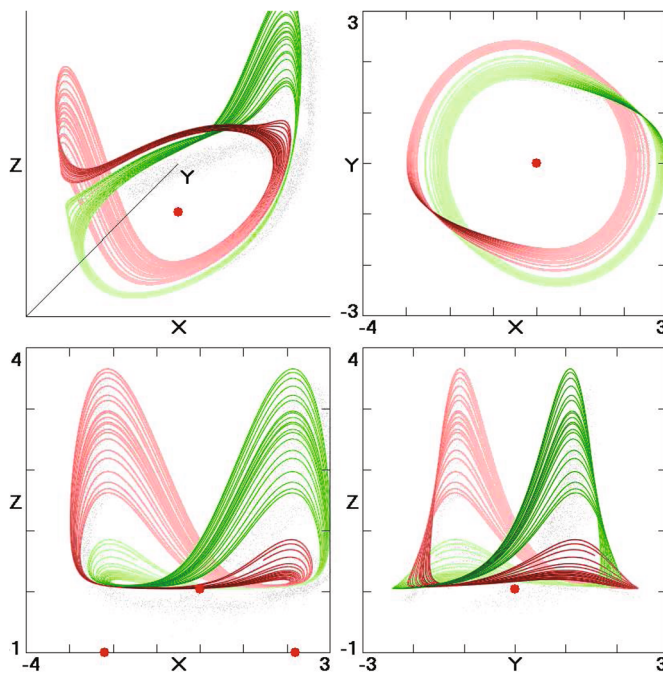


Fig. 4. Four views of the rotationally-symmetric pair of Rössler attractors for $(a, b, c) = (0.2, 0.2, 4.6)$ with initial conditions $(\pm 1, 0, 0)$ in Eq. (2). The green and red attractors correspond to two symmetric initial conditions, and the equilibrium points are shown as red dots.

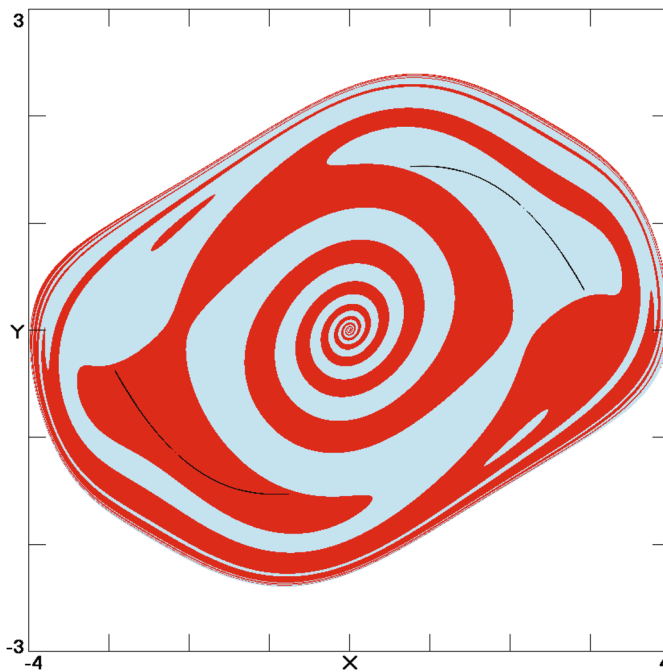


Fig. 5. Cross section for $z = 2$ of the basins of attraction for the symmetric pair of strange attractors (light blue and red) of system (2) at $a = b = 0.2, c = 4.6$.

where a symmetric limit cycle is born around $c = 5.4$ that then undergoes a pitchfork bifurcation around $c = 5.6$, forming a symmetric pair of limit cycles that period-double into a symmetric pair of strange attractors in the vicinity of $c = 5.8$ that then merge into a single symmetric strange attractor around $c = 5.9$.

Note that even though the equations have rotational symmetry, it does not follow that the solutions are multistable with a symmetric pair of coexisting attractors. On the contrary, as examples, the piecewise rotationally-symmetric systems [17] have a single global symmetry as does the Lorenz attractor [16]. Similarly, the symmetry brings the possibility of an amplitude controller. However, we cannot claim that all the symmetric systems have independent amplitude parameters because that symmetry requires only a balance of polarity rather than necessarily a balance of amplitude, in which case a signum operation can satisfy this condition even though the amplitude information is removed.

For example, based on system (1), we design a reflection invariant system [14], which is invariant under the transformation $(x, y, z) \rightarrow (x, y, -z)$, corresponding to symmetry about the $z = 0$ plane. To balance the polarity, we apply a signum function, which leads to the system

$$\begin{aligned}\dot{x} &= -y - z^2 \\ \dot{y} &= x + ay \\ \dot{z} &= b\text{sgn}(z) + z(x - c).\end{aligned}\tag{4}$$

When $a = b = 0.2, c = 2.5$, system (4) has a coexisting symmetric pair of single-scroll strange attractors as shown in Fig. 6 with smooth basins of attraction as shown in Fig. 7. System (4) is different from the equivariant double cover with reflection symmetry of the Rössler system proposed in [18]. The corresponding Lyapunov exponents of the two coexisting attractors are $(0.0583, 0, -2.2601)$, and the Kaplan-Yorke dimension is $D_{KY} = 2.0258$. There is a well-known difficulty when calculating Lyapunov exponents for systems that involve discontinuous functions such as the signum. This problem arises because of the abrupt change in the direction of the flow vector at the discontinuity and the difficulty of maintaining the correct orientation of the Lyapunov vectors. Although there is a proper procedure for correcting this problem [19], we use here a simpler method in which $\text{sgn}(z)$ is replaced by a smooth approximation given by $\tanh(Nz)$ with N sufficiently large that the calculated Lyapunov exponents are independent of its value [20]. System (4) has four equilibrium points, $(2.4428, -12.2139, \pm 3.4948)$ and $(0.0013, -0.0064, \pm 0.0800)$ with eigenvalues $(0.1899, -0.0236 \pm 5.0423i)$ and $(-2.4942, 0.0978 \pm 0.9956i)$, respectively, which are two different kinds of spiral saddles. The two pairs of equilibrium points are symmetric about the $z = 0$ plane. The signum function of the variable z in the third dimension prevents the coefficient of the quadratic term z^2 in the first dimension from being an amplitude control parameter unless the $\text{sgn}(z)$ function is replaced by z .

3 Multistability in symmetric systems with total amplitude control

For constructing a symmetric system with a total amplitude parameter, the balance of polarity must be achieved, and this leads to an inversion invariant system with respect to changes in all three variables (also called parity invariant) [14]. Such a system is invariant under the transformation $(x, y, z) \rightarrow (-x, -y, -z)$, corresponding to symmetry about the origin. Kremlivsky also constructed an inversion invariant Rössler system using a nonlinear term zx^2 to cancel the extra polarity [21]. Here we introduce an absolute-value function to cancel the redundant polarity in the third dimension of system (1) and introduce a linear variable to substitute for the constant

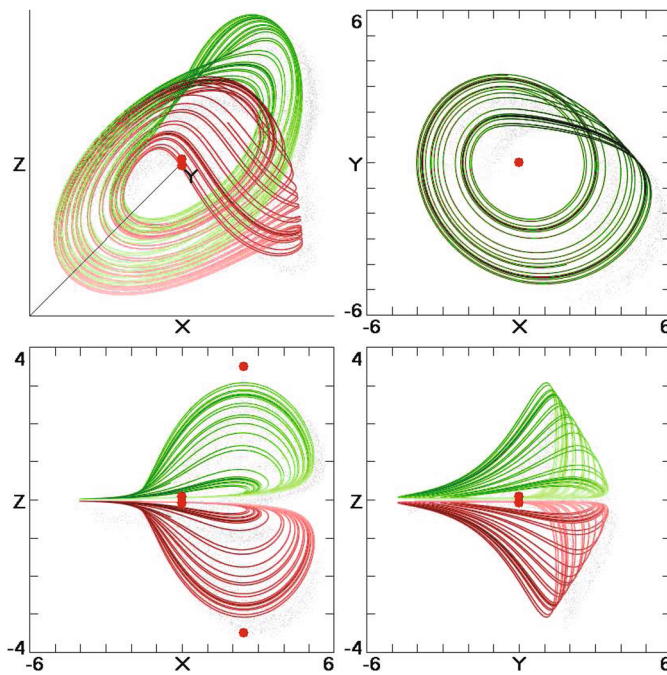


Fig. 6. Four views of the reflection-invariant Rössler attractors for $(a, b, c) = (0.2, 0.2, 2.5)$ with initial conditions $(0, 0, \pm 1)$ in Eq. (4). The green and red attractors correspond to two symmetric initial conditions, and the four equilibrium points are shown as red dots.

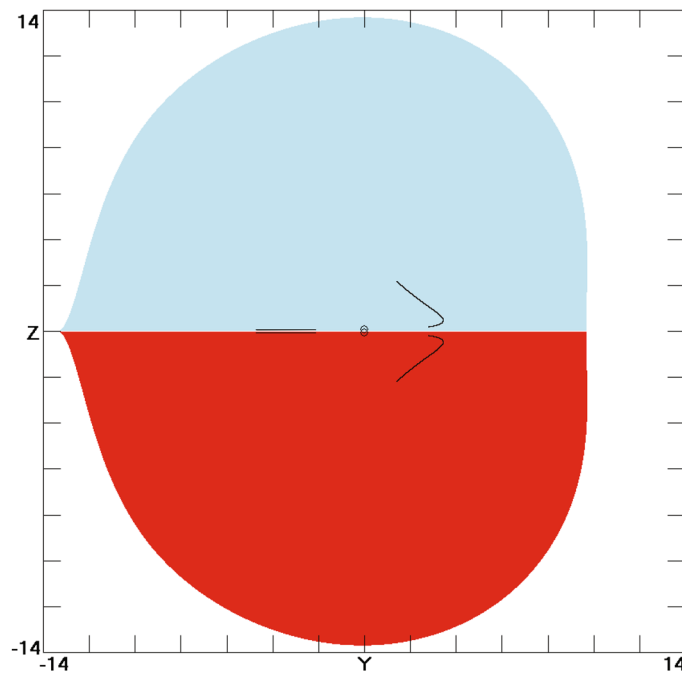


Fig. 7. Cross section for $x = 0.00128$ of the basins of attraction (light blue and red) for the symmetric pair of strange attractors for system (4) at $a = b = 0.2, c = 2.5$.

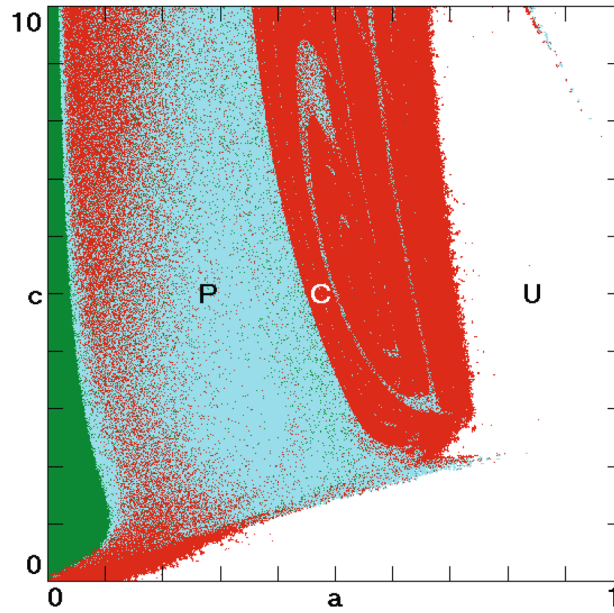


Fig. 8. Regions of various dynamical behaviors for system (5) as a function of the bifurcation parameters a and c with $b = 0.2$. The chaotic and transiently chaotic regions (C) are shown in red, the periodic regions (P) are shown in cyan, the stable equilibrium regions (S) are shown in green, and the unbounded regions (U) are shown in white.

and compensate for the polarity so as to keep the balance, giving the system

$$\begin{aligned}\dot{x} &= -y - z \\ \dot{y} &= x + ay \\ \dot{z} &= bx + x|z| - cz.\end{aligned}\quad (5)$$

System (5) is an inversion-invariant system. The dynamic regions of system (5) in the parameter space of (a, c) at $b = 0.2$ are shown in Fig. 8. When $a = 0.5, b = 0.2, c = 5.7$, it shows chaotic behavior with an attractor as shown in Fig. 9. The corresponding Lyapunov exponents are $(0.1597, 0, -1.9865)$, and the Kaplan-Yorke dimension is $D_{KY} = 2.0804$. System (5) has three equilibrium points, $(0, 0, 0)$ and $(\pm 5.6, \mp 11.2, \pm 11.2)$ with eigenvalues $(-5.6657, 0.2328 \pm 0.9665i)$ and $(0.4526, -0.0263 \pm 3.5175i)$, respectively, which are two different kinds of spiral saddles. The transformation adds one equilibrium point, and the equilibria are symmetric with respect to the origin.

System (5) has one independent total amplitude parameter m in the $x|z|$ term,

$$\begin{aligned}\dot{x} &= -y - z \\ \dot{y} &= x + ay \\ \dot{z} &= bx + mx|z| - cz.\end{aligned}\quad (6)$$

To show this, let $x = u/m, y = v/m, z = w/m$ to obtain new equations in the variables u, v, w that are identical to Eq. (5). Therefore, the coefficient m controls the amplitude of the variables x, y and z according to $1/m$. Note that since system (5) has only one nonlinear term, an independent total amplitude parameter can be obtained without any other coordinated control as is necessary if there is more than one nonlinear term.

When $a = 0.5, b = 0.2, c = 4$, system (5) has a symmetric pair of coexisting strange attractors as shown in Fig. 10 with basins of attraction as shown in Fig. 11.

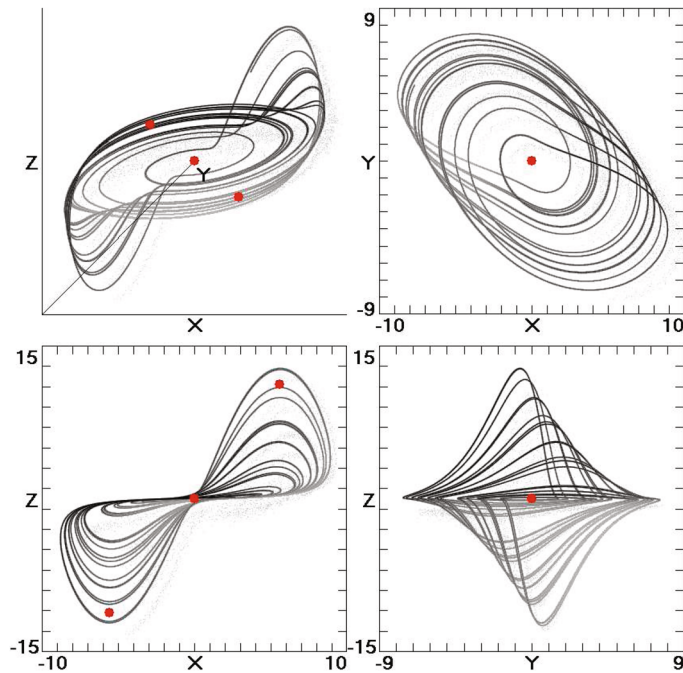


Fig. 9. Four views of the inversion-symmetric Rössler attractor for $(a, b, c) = (0.5, 0.2, 5.7)$ with initial conditions $(1, 0, 0)$ in Eq. (5). The three equilibrium points are shown as red dots.

The basins of attraction for the two chaotic attractors are indicated by light blue and red, respectively. The basins have the expected symmetry about the origin and an intricate fractal structure. With a change of parameter c , the two coexisting strange attractors merge into one like the attractor shown in Fig. 9. The corresponding Lyapunov exponents of the two coexisting attractors are $(0.1007, 0, -0.8982)$, and the Kaplan-Yorke dimension is $D_{KY} = 2.1121$.

In addition, considering the balance of polarity based on system (2), two other inversion-invariant systems can be derived as described by

$$\begin{aligned}\dot{x} &= -y - xyz \\ \dot{y} &= x + ay \\ \dot{z} &= bx + z(x^2 - c)\end{aligned}\tag{7}$$

$$\begin{aligned}\dot{x} &= -y - yz^2 \\ \dot{y} &= x + ay \\ \dot{z} &= bx + z(x^2 - c).\end{aligned}\tag{8}$$

When $a = b = 0.2$, these systems have a symmetric pair of coexisting strange attractors at $c = 5.5$ and $c = 2.25$, respectively, as shown in Figs. 12 and 13. The corresponding Lyapunov exponents for the two pairs of coexisting attractors are $(0.0509, 0, -2.7365)$ and $(0.0938, 0, -0.4278)$, and the Kaplan-Yorke dimensions are 2.0186 and 2.2193, respectively. Note that the coefficient of any cubic term in system (7) or (8) now is not an independent amplitude parameter unless the coefficient of the other cubic term varies proportionally [13]. The new introduced coefficient h in both of the cubic terms will control the amplitude of all the variables according to $1/\sqrt{h}$.

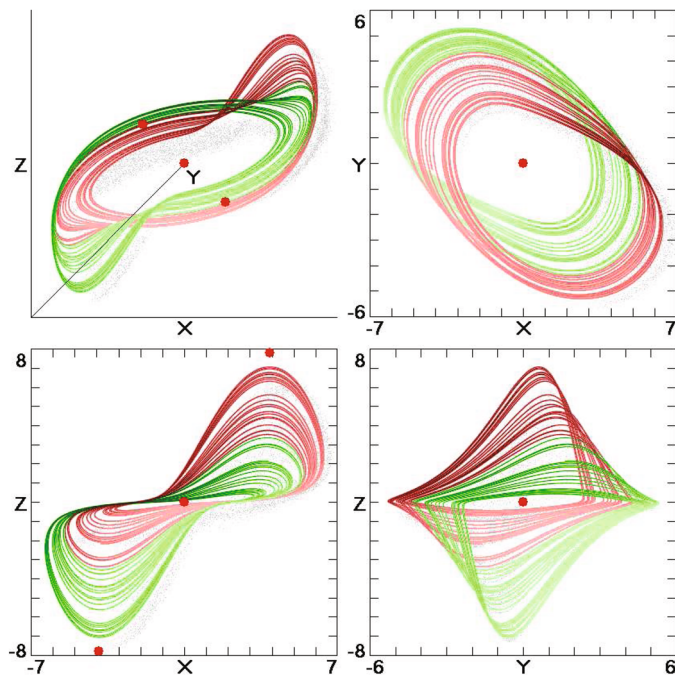


Fig. 10. Four views of the inversion-symmetric Rössler attractors for $(a, b, c) = (0.5, 0.2, 4)$ with initial conditions $(\pm 1, 0, 0)$ in Eq. (5). The green and red attractors correspond to two symmetric initial conditions, and the three equilibrium points are shown as red dots.

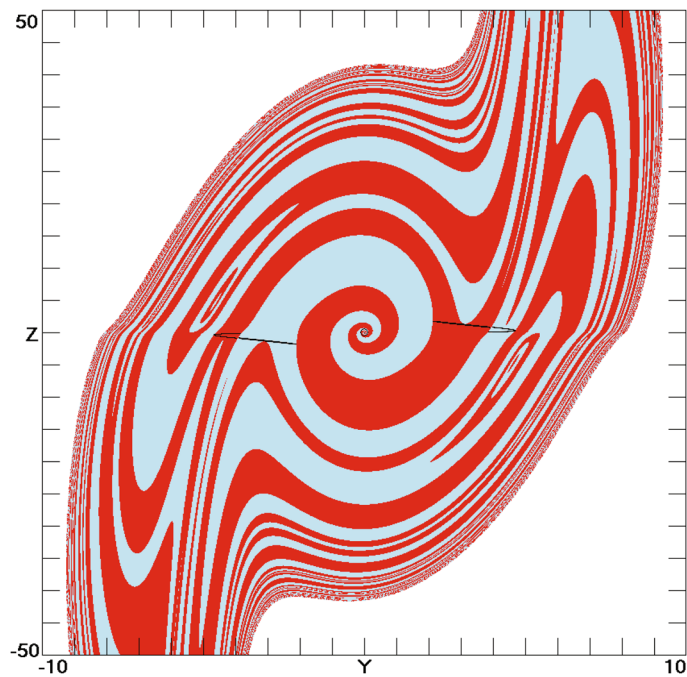


Fig. 11. Cross section for $x = 0$ of the basins of attraction for the symmetric pair of strange attractors (light blue and red) for system (5) with $a = 0.5, b = 0.2, c = 4$.

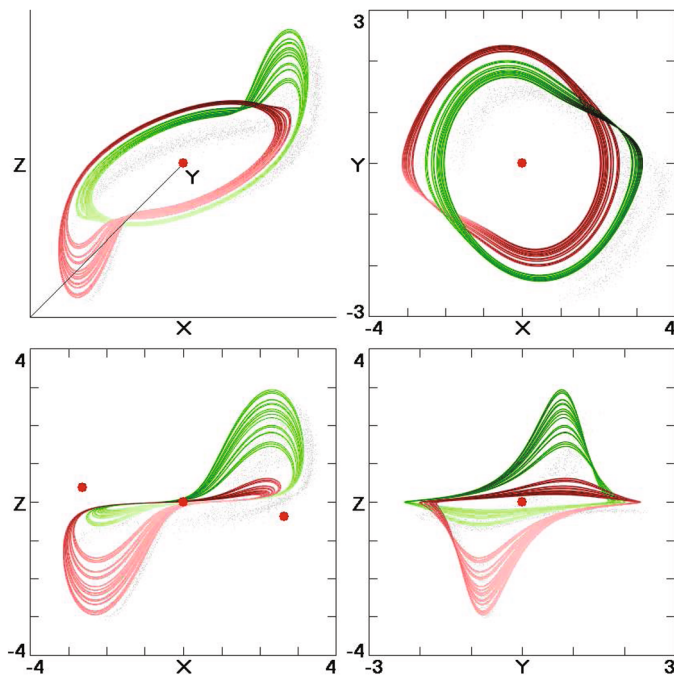


Fig. 12. Four views of the inversion-symmetric Rössler attractors for $(a, b, c) = (0.2, 0.2, 5.5)$ with initial conditions $(\pm 1, 0, 0)$ in Eq. (7). The green and red attractors correspond to two symmetric initial conditions, and the three equilibrium points are shown as red dots.

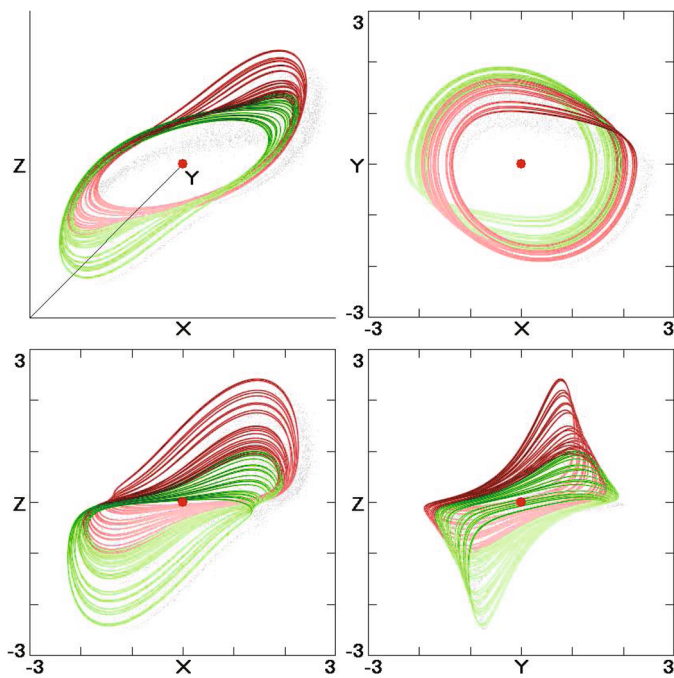


Fig. 13. Four views of the inversion-symmetric Rössler attractors for $(a, b, c) = (0.2, 0.2, 2.25)$ with initial conditions $(\pm 1, 0, 0)$ in Eq. (8). The green and red attractors correspond to two symmetric initial conditions, and the single equilibrium point at the origin is shown as a red dot.

Otherwise, to realize amplitude control with an independent parameter, a nonlinear equation with only one term of different degree should be derived. Such a system is

$$\begin{aligned}\dot{x} &= -y - |z|\operatorname{sgn}(y) \\ \dot{y} &= x + ay \\ \dot{z} &= bx + z(x^2 - c)\end{aligned}\tag{9}$$

where the coefficient of the cubic term can control the amplitude of all the variables according to $h^{-1/3}$. When $c = 4.25$, system (9) has a symmetric pair of strange attractors that resemble those in the cubic system (8) but with discontinuities in the direction of the flow. The introduction of the piecewise linear element will shrink the region of parameter space where multistability occurs, but coexisting strange attractors still occur in a narrow parameter region.

4 Asymmetric coexisting attractors

In addition to the symmetric pairs of strange attractors resulting from the symmetry of the above equations, there are regions of parameter space that admit symmetric pairs of limit cycles, asymmetric pairs of attractors of the same type, and asymmetric pairs of attractors of different types. Even the regular Rössler system (1) has regions of coexisting attractors. Figure 14(a) shows two coexisting interlinked strange attractors with Lyapunov exponents $(0.0398, 0, -3.6120)$ and $(0.0346, 0, -3.8953)$, and Fig. 14(b) shows a limit cycle with Lyapunov exponents $(0, -0.2063, -1.8803)$ coexisting and interlinked with a strange attractor with Lyapunov exponents $(0.0549, 0, -2.3166)$ for system (1). In addition, there are regions where limit cycles of different periods coexist. Attempts to find parameters where a strange attractor coexists with a stable equilibrium in system (1) were unsuccessful.

The symmetric systems (2) through (8) also exhibit asymmetric coexisting attractors for certain values of the parameters. For example, Fig. 14(c) shows a symmetric limit cycle with Lyapunov exponents $(0, -0.1686, -1.3144)$ coexisting with a symmetric strange attractor with Lyapunov exponents $(0.1936, 0, -1.6127)$, and Fig. 14(d) shows a symmetric pair of limit cycles with Lyapunov exponents $(0, -0.0179, -1.8236)$ coexisting with a symmetric pair of strange attractors with Lyapunov exponents $(0.0317, 0, -1.7427)$ in system (2). The basins of attraction for those coexisting asymmetric attractors are also asymmetric, which are different from the basins of the coexisting symmetric ones. Note that all of the attractors for these systems appear to be self-excited rather than hidden [22–24] in the sense that their basin of attraction includes the neighborhood of one or more of the unstable equilibrium points.

5 Discussion and conclusions

Multistability and amplitude control unify in systems with symmetry. Coexisting attractors may be born in symmetric systems, and one independent amplitude parameter may exist in the coefficient of the term with different degree. By different alterations of the Rössler system, three different kinds of symmetry are derived, which show that symmetrization is a valid path to lead to multistability and amplitude control. Symmetry provides an independent amplitude control parameter in chaotic systems, which is good for engineering applications. However, the symmetry allows multistability, which may influence the amplitude control resulting in an undesirable “hop” among the coexisting attractors unless the initial conditions are modified proportionally.

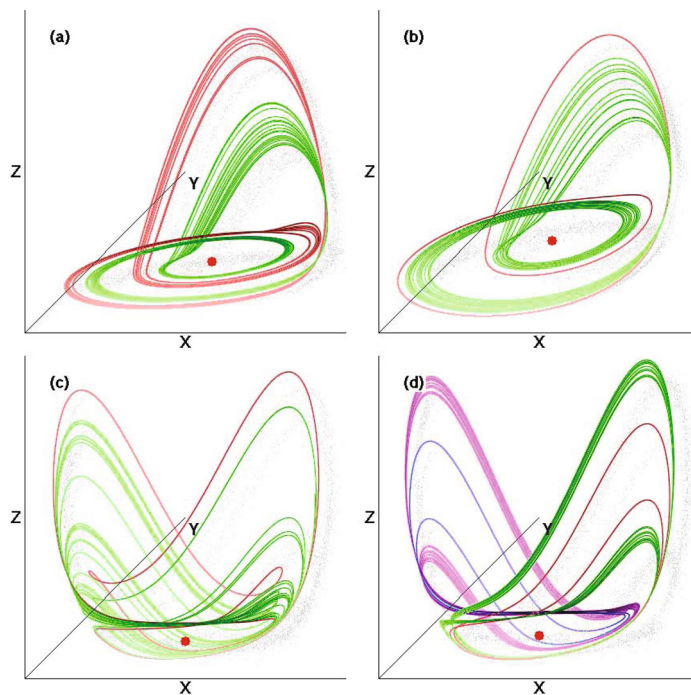


Fig. 14. Coexisting attractors in the original and symmetric Rössler systems. (a) System (1) with $(a, b, c) = (0.29, 0.14, 4.52)$ and initial conditions $(2, 6, 0.75)$ and $(-3, 0, 0.04)$ shows two coexisting asymmetric strange attractors. (b) System (1) with $(a, b, c) = (0.41, 0.72, 3.12)$ and initial conditions $(1, 2.4, 1)$ and $(0, -2.3, 0.2)$ shows an asymmetric limit cycle coexisting with an asymmetric strange attractor. (c) System (2) with $(a, b, c) = (0.39, 2.23, 4.71)$ with initial conditions $(2.3, 0, 4.6)$ and $(0, -1, 5.5)$ shows a symmetric limit cycle coexisting with a symmetric strange attractor. (d) System (2) with $(a, b, c) = (0.34, 1.7, 5.03)$ with initial conditions $(\pm 0.4, \pm 1, 6.6)$ and $(\pm 2.8, 0, 2.8)$ shows a symmetric pair of limit cycles coexisting with a symmetric pair of strange attractors.

This work was supported financially by the National Natural Science Foundation of China (Grant No. 61401198), the NUAA Fundamental Research Funds (No. NS2013025), the Jiangsu Overseas Research and Training Program for University Prominent Young and Middle-aged Teachers and Presidents, the 4th 333 High-level Personnel Training Project (Su Education [2013] No. 60) and the National Science Foundation for Postdoctoral General Program and Special Founding Program of People's Republic of China (Grant No. 2011M500838 and Grant No. 2012T50456) and Postdoctoral Research Foundation of Jiangsu Province (Grant No. 1002004C).

References

1. J.C. Sprott, X. Wang, G. Chen, *Int. J. Bifurcat. Chaos* **23**, 1350093 (2013)
2. C. Li, J.C. Sprott, W. Thio, *J. Exp. Theor. Phys.* **118**, 494 (2014)
3. C. Li, J.C. Sprott, *Int. J. Bifurcat. Chaos* **24**, 1450034 (2014)
4. C. Li, J.C. Sprott, *Int. J. Bifurcat. Chaos* **23**, 1350199 (2013)
5. J.C. Sprott, *Phys. Lett. A* **378**, 1361 (2014)
6. B. Blazejczyk-Okolewska, T. Kapitaniak, *Chaos, Solitons Fractals* **9**, 1439 (1998)
7. A. Chudzik, P. Perlikowski, A. Stefanski, T. Kapitaniak, *Int. J. Bifur. Chaos* **21**, 1907 (2011)

8. C. Li, J.C. Sprott, *Nonlinear Dyn.* **78**, 2059 (2014)
9. W. Hu, Z. Liu, *IET Signal Processing* **2**, 423 (2008)
10. L.M. Pecora, *Phys. Rev. Lett.* **64**, 821 (1990)
11. G. Kolumban, M.P. Kennedy, L.O. Chua, *IEEE Trans. Circuits Syst.- I Fund. Theor. Appl.* **45**, 1129 (2002)
12. C. Li, J.C. Sprott, *Phys. Lett. A* **378**, 178 (2014)
13. C. Li, J.C. Sprott, *Nonlinear Dyn.* **73**, 1335 (2013)
14. J.C. Sprott, *Int. J. Bifurcat. Chaos* **24**, 1450009 (2014)
15. O.E. Rössler, *Phys. Lett. A* **57**, 397 (1976)
16. E.N. Lorenz, *J. Atmos. Sci.* **20**, 130 (1963)
17. C. Li, J.C. Sprott, W. Thio, H. Zhu, *IEEE Trans. Circuits Syst. -II: Exp. Briefs* **61**, 977 (2014)
18. R. Gilmore, C. Letellier, *The Symmetry of Chaos* (Oxford University Press, Inc. 2007), p. 71
19. W.J. Grantham, B. Lee, *Dynam. Contr.* **3**, 159 (1993)
20. R.F. Gans, *J. Sound Vibr.* **188**, 75 (1995)
21. C. Letellier, R. Gilmore, *Phys. Rev. E* **63**, 016206 (2000)
22. G.A. Leonov, V.I. Vagaitsev, N.V. Kuznetsov, *Phys. Lett. A* **375**, 2230 (2011)
23. G.A. Leonov, V.I. Vagaitsev, N.V. Kuznetsov, *Physica D* **241**, 1482 (2012)
24. G.A. Leonov, N.V. Kuznetsov, *Int. J. Bifurcat. Chaos* **25**, 1330002 (2013)